Comparing measurements of $g^{(2)}(0)$ performed with different coincidence detection techniques

M. Beck

Department of Physics, Whitman College, Walla Walla, Washington 99362, USA
beckmk@whitman.edu

Received June 22, 2007; revised August 28, 2007; accepted September 17, 2007;
posted October 11, 2007 (Doc. ID 84422); published November 14, 2007

I present measurements of the degree of second-order coherence $g^{(2)}(0)$ for spontaneous parametric downconversion fields and discuss the differences between two-detector (unconditional) and three-detector (conditional) measurements of $g^{(2)}(0)$. An emphasis is placed on comparing measurements made using time-to-amplitude converters (TACs) to those made using a logic circuit, illustrating how the TAC measurements are adversely influenced by dead time effects. Finally, I show how the detrimental effects of dead time when using TACs can be mitigated by renormalizing the measurement results. © 2007 Optical Society of America

OCIS codes: 270.5290, 030.5290, 030.5260.

1. INTRODUCTION

The degree of second-order (temporal) coherence $g^{(2)}(\tau)$ has a long and important history in quantum optics. Indeed, it can be argued that measurements performed by Hanbury Brown and Twiss of quantities related to the degree of second-order coherence are what stimulated the creation of the modern field of quantum optics [1,2]. One of the first experiments to observe a purely quantum-mechanical effect in an optical field was the observation of photon antibunching, in which the quantity of interest is $g^{(2)}(\tau)$ [3,4]. Since then measurements of $g^{(2)}(\tau)$ (and closely related quantities) have played an important role in quantum optics (see, for example, [5–12]).

Here I present expressions for $g^{(2)}(0)$ in terms of experimentally measurable quantities, accounting for the real experimental imperfection of dead time effects. The special case of $\tau=0$ is important, because $g^{(2)}(0)$ can be used to distinguish between classical and quantum fields; classical wave theory predicts that $g^{(2)}(0)\geq 1$, whereas quantum mechanics allows $g^{(2)}(0)<1$. I make a distinction between two- and three-detector measurements of $g^{(2)}(0)$ (for clarity I refer to these as $g^{(2)}_{2D}(0)$ and $g^{(2)}_{3D}(0)$, respectively.) In two-detector measurements the field to be measured impinges on a beam splitter, and the two output ports are monitored with photon-counting detectors; I refer to this as an unconditional measurement. Three-detector measurements are conditional, because the two detectors monitoring the beam splitter outputs are gated by (conditioned on) detection events at a third detector. This third detector monitors a second field, so $g^{(2)}_{3D}(0)$ depends not only on the properties of the field incident on the beam splitter but also on the correlations between this field and the field incident on the third detector.

As will be seen below, dead time in the coincidence determination can dramatically degrade the experimental measurements, yielding results that differ considerably from the usual theoretical predictions. I demonstrate two different techniques for overcoming this problem. The preferred method is to reduce the amount of dead time and hence improve the quality of the data. This is illustrated by comparing two different coincidence detection techniques: one using time-to-amplitude converters (TACs), which sufferers from dead time problems, and the other using a logic circuit that has essentially no dead time. If one does not have access to coincidence detection equipment with short dead time, I show that it is possible to renormalize the data in such a way as to improve the agreement between the measurements and the theoretical predictions.

2. THEORY

One typically measures $g^{(2)}(\tau)$ of a beam of light by sending the beam onto a beam splitter and measuring the correlations between the reflected and transmitted output intensities $I_R(t)$ and $I_T(t)$; see Fig. 1. Classically $g^{(2)}(\tau)$ of the incident beam is given by the normalized correlations of the output beams [13]:

$$g^{(2)}(\tau)=\frac{\langle I_T(t+\tau)I_R(t)\rangle}{\langle I_T(t+\tau)\rangle\langle I_R(t)\rangle}, \tag{1}$$

where the brackets indicate a time average, which may be replaced by an ensemble average for stationary fields. For classical waves the intensities of the transmitted and reflected beams are related to the input intensity by $I_T(t)=TI_I(t)$ and $I_R(t)=RI_I(t)$, where T and R are the intensity transmission and reflection coefficients of the beam splitter. Because of this fact, $g^{(2)}(t)$ can be rewritten in terms of the incident intensity as

$$g^{(2)}(\tau)=\frac{\langle I_I(t+\tau)I_I(t)\rangle}{\langle I_I(t+\tau)\rangle\langle I_I(t)\rangle}. \tag{2}$$

Note that this expression is independent of the splitting ratio of the beam splitter (although in practice one cannot get too close to a 100/0 or 0/100 splitting ratio, because

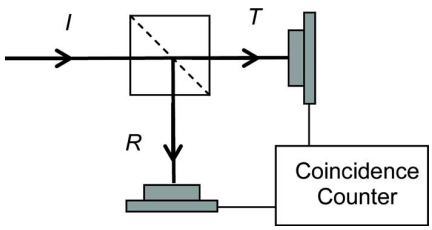

Fig. 1. (Color online) Coincidence measurement. The incident (I) beam is split into transmitted (T) and reflected (R) beams at a 50/50 beamsplitter. Detections at T and R are examined to see whether they occur simultaneously.

then $g^{(2)}(t)$ becomes the ratio of two very small numbers, and the expression is not well behaved for experimental data.) For $\tau=0$ Eq. (2) becomes

$$g^{(2)}(0)=\frac{\langle I_I^2(t)\rangle}{\langle I_I(t)\rangle^2}. \tag{3}$$

The Cauchy–Schwartz inequality applied to this expression yields the result that for classical waves $g^{(2)}(0)\geq 1$.

Equation (1) is a classical expression; the quantum expression has the intensities replaced by their corresponding operators [13,14]:

$$g^{(2)}(\tau)=\frac{\langle :\hat{I}_T(t+\tau)\hat{I}_R(t):\rangle}{\langle \hat{I}_T(t+\tau)\rangle\langle \hat{I}_R(t)\rangle}, \tag{4}$$

where the colons indicate that the operators inside must be normally ordered and time ordered. If light in an n-photon Fock state is incident on the beam splitter, it is straightforward to show that $g^{(2)}(0)=(n-1)/n$. For a Fock state it is always true that $g^{(2)}(0)<1$, which clearly violates the classical wave inequality. The maximum violation of this inequality occurs for a single-photon Fock state, for which $g^{(2)}(0)=0$.

A. Two-Detector Measurements of $g^{(2)}(0)$

In an experiment one does not directly measure the intensity, so it is necessary to relate the expressions for $g^{(2)}(0)$ given above to experimentally measured quantities. It can be shown that when $g^{(2)}(0)$ is measured using photoelectric detection, it is written in terms of the probabilities of individual photodetections as

$$g_{2D}^{(2)}(0)=\frac{P_{TR}}{P_T P_R}, \tag{5}$$

where $P_T(P_R)$ is the probability of a detection at detector $T(R)$ in a short time interval Δt, and P_{TR} is the joint probability of making detections at both T and R in the same time interval [14]. The subscript $2D$ on $g^{(2)}(0)$ in Eq. (5) emphasizes that this expression is valid for measurements performed with two detectors.

Equation (5) is obtained using either the semiclassical or the fully quantum mechanical theory of photodetection—the difference between the two being how the probabilities are calculated. It remains the case that for classical light $g_{2D}^{(2)}(0)\geq 1$, whereas nonclassical light allows $g_{2D}^{(2)}(0)<1$.

Experimentally, how does one measure $g_{2D}^{(2)}(0)$? To answer this I must explain how the probabilities in Eq. (5) are determined from measured count rates. For example, the probability of a detection at detector T within Δt is simply given by the average rate of detections at T, R_T, multiplied by Δt. The average rate is just the total number of detections N_T divided by the total counting time ΔT. The probabilities for R detections and TR coincidences are given similarly:

$$P_T=R_T\Delta t=\left(\frac{N_T}{\Delta T}\right)\Delta t,\quad P_R=R_R\Delta t=\left(\frac{N_R}{\Delta T}\right)\Delta t,$$

$$P_{TR}=R_{TR}\Delta t=\left(\frac{N_{TR}}{\Delta T}\right)\Delta t. \tag{6}$$

These equations are valid as long as the detection probabilities are much less than 1. Substituting these probabilities into Eq. (5) yields

$$g_{2D}^{(2)}(0)=\frac{N_{TR}}{N_T N_R}\left(\frac{\Delta T}{\Delta t}\right). \tag{7}$$

This same expression can be derived more rigorously using results found in [14].

It was mentioned above that $g^{(2)}(0)$ is independent of the splitting ratio of the beam splitter, but it is also independent of the detection efficiencies of the detectors [14]. This independence on detection efficiency arises because the number of coincidence detections in the numerator of Eq. (7) is related to the intensities by the product of the detection efficiencies at T and R, but the denominator has the same dependence; the detection efficiencies thus cancel out. This is one reason why photon antibunching was one of the first intrinsically quantum field effects to be observed—it could be seen with low efficiency detectors, whereas low efficiency detection frequently masks quantum effects.

B. Three-Detector Measurements of $g^{(2)}(0)$

As described above, $g_{2D}^{(2)}(0)$ is measured for a single beam incident on a beam splitter and using two detectors, labeled T and R. However, experiments are frequently performed in which a second source beam is incident on a third detector that is used as a gate (and correspondingly labeled G), as shown in Fig. 2 [5,15]. Figure 2 depicts our experimental arrangement (described in more detail below); for the purposes of the discussion here, the salient point is that two beams emerge from the source (here a downconversion crystal, labeled DC). One beam is detected at G, while the other goes to a beam splitter and is detected at T and R. Since the T and R detections are conditioned on a detection at G, it is reasonable to expect the probabilities in Eq. (5) to be further conditioned upon a gate detection, and hence this expression becomes

$$g_{3D}^{(2)}(0)=\frac{P_{GTR}}{P_{GT}P_{GR}}. \tag{8}$$

Here P_{GTR} is the probability of obtaining a threefold coincidence between detectors T, R, and G in the time interval Δt. The subscript $3D$ in Eq. (8) emphasizes that this ex-

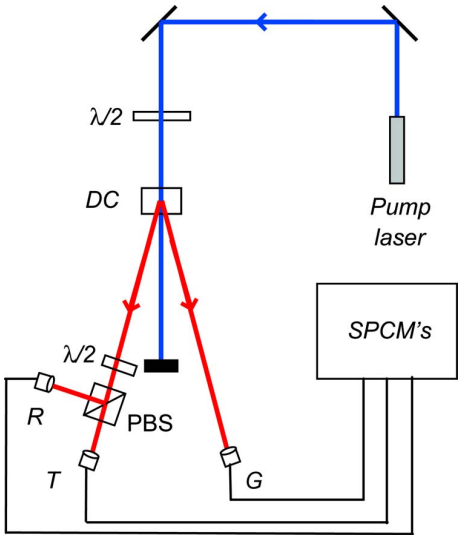

Fig. 2. (Color online) Experimental apparatus. Major components include the pump laser; the downconversion crystal (DC); the half-wave plate (λ/2); the polarizing beam splitter (PBS); the single-photon counting modules (SPCMs); and gating, transmission-side, and reflection-side collection optics (G, T, and R). Optical fibers direct the light from G, T, and R to their corresponding SPCMs. The coincidence electronics and counting occur after the SPCMs.

pression is valid for three-detector measurements of $g^{(2)}(0)$. I refer to such measurements as being conditional because of the conditioning provided by the gate detector.

Because in three-detector measurements the gate detections can be used as the number of trials, it is possible to normalize the probabilities in Eq. (8) differently from those in Eq. (5). The probabilities are given by the number of coincidences divided by the number of trials, which is equal to the number of gate detections:

$$P_{GTR} = \frac{N_{GTR}}{N_G}, \quad P_{GT} = \frac{N_{GT}}{N_G}, \quad P_{GR} = \frac{N_{GR}}{N_G}, \tag{9}$$

where, given a specified time window, N_{GT} (N_{GR}) is the number of simultaneous photocounts at detector T (R) and detector G, N_{GTR} is the number of threefold coincidences, and N_G is the number of singles counts at detector G. Note that with these expressions it is not necessary to make specific reference to the coincidence window or total counting time. Using Eq. (9), the experimentally determined $g_{3D}^{(2)}(0)$ can be rewritten as

$$g_{3D}^{(2)}(0) = \frac{N_{GTR} N_G}{N_{GT} N_{GR}}. \tag{10}$$

Again, this quantity is independent of the detection efficiencies, because when relating the number of detected photons to the intensities both the numerator and denominator depend linearly on the efficiencies at T and R and quadratically on the efficiency at G (see also [5]).

In order to avoid confusion, I will comment here on the differences between two- and three-detector measurements. The two-detector measurement $g_{2D}^{(2)}(0)$ most closely represents a measurement of the "true" definition of $g^{(2)}(0)$ of a light beam. The three-detector measurement $g_{3D}^{(2)}(0)$ represents a conditional $g^{(2)}(0)$, where the conditioning is done using measurements on a second beam—in some sense one may think of Eqs. (8)–(10) as defining what is meant by this conditional measurement of $g^{(2)}(0)$. Conditioning is useful in cases where one has two beams that are correlated in intensity, and one wishes to measure $g^{(2)}(0)$ of one beam conditioned on the presence of a photon in the second beam. An important example is the case of spontaneous downconversion, where detection of a photon in the idler beam projects the signal beam into a single-photon state (now often referred to as heralded single-photon generation) [16].

My definition of $g_{3D}^{(2)}(0)$ is the same as that of the α parameter defined by Grangier *et al.*: $g_{3D}^{(2)}(0) = \alpha$ [5,17]. Using the semiclassical model of detection, it was proved by Grangier *et al.* that $g_{3D}^{(2)}(0) \geq 1$ for a classical source, so a measurement of $g_{3D}^{(2)}(0) < 1$ is at odds with the classical wave theory of light. For photon pairs produced from a cascade decay in calcium, Grangier *et al.* were able to measure $g_{3D}^{(2)}(0) = 0.18 \pm 0.06$ [5]. This was an important experiment demonstrating that conditional measurements could produce nonclassical light.

Because two- and three-detector measurements of $g^{(2)}(0)$ both yield the same inequality for classical fields: $g_{2D}^{(2)}(0) \geq 1$ and $g_{3D}^{(2)}(0) \geq 1$, it's easiest to simply say that for classical fields $g^{(2)}(0) \geq 1$.

3. DEAD TIME EFFECTS

Dead time refers to the fact that once a photon is detected, certain instruments require time to reset themselves. During this dead time further counts cannot be processed. The single-photon detection rates in the experiments described here are on the order of 10^6 cps (counts per second) or less. The dead time of the detectors is 50 ns, so significantly larger count rates would be needed for detector dead time to have a significant effect.

However, the dead time in the TACs frequently used to measure coincidences is on the order of 1 μs, so this can influence the results. For a periodic train of photons, it is possible to operate a TAC at rates approaching 10^6 cps. However, if the photons are produced at random times, even if the average time between photons is more than 1 μs, there is some probability that photons are separated by less than this and coincidences will be missed.

These missed coincidences will effect measurements of $g_{2D}^{(2)}(0)$ and $g_{3D}^{(2)}(0)$. For example, consider Eq. (7). It was stated above that detector inefficiencies affect the numerator and denominator of Eq. (7) in the same way so as to cancel out and have no net effect. However, dead-time effects in the coincidence measurement reduce the measured coincidences in the numerator of Eq. (7) but have no effect on the singles detections in the denominator. Thus, if dead-time effects in coincidence determination are important, we expect experimental measurements of $g_{2D}^{(2)}(0)$ to yield smaller values than we would otherwise expect.

Fortunately TACs give the experimenter a way to measure the effects of dead time. Each TAC has an output labeled VALID START (VS). Every time a START pulse *successfully* initiates a conversion event, there is a VS output pulse. For example, suppose that one START pulse ini-

tiates a conversion event; for this conversion event the TAC outputs a VS. If a second START pulse arrives within the dead time, it cannot initiate a conversion event, and no VS pulse is output. Since this second START pulse does not initiate a conversion event, it cannot contribute to the measured coincidences. This is what leads to missed coincidences using TACs.

As dead time becomes more important, the number of VSs becomes a smaller fraction of the number of STARTs. This can be visualized, for example, by plotting the rate of VS pulses due to the gate $R_{G\ vs}$ on the TAC measuring GT coincidences versus the rate of START pulses R_G, as shown in Fig. 3. For a periodic train of STARTs (circles in Fig. 3) the VSs track the STARTs up to about 9×10^5 cps. Above this rate the pulses are closer together than the dead time, so only every other pulse is measured. For random downconversion events (triangles in Fig. 3), however, the number of VSs are less than the number of STARTs, and the discrepancy increases as the count rate increases. At a rate of 10^5 cps the discrepancy is not large (only about 10%), but it rapidly increases at higher rates. However, there is a way to correct the measurements to account for this error. The key to doing this is to realize that when measuring $g^{(2)}_{2D}(0)$ or $g^{(2)}_{3D}(0)$, only START pulses that trigger a VS can possibly contribute to a measured coincidence.

First consider the effects on $g^{(2)}_{2D}(0)$. When measuring the coincidences N_{TR}, it is the T detector that serves as the START pulse. Only detections at T that trigger a VS can possibly contribute to the N_{TR} coincidences, so the proper normalization in Eq. (7) should involve $N_{T\ vs}$, not N_T. This means the corrected expression for $g^{(2)}_{2D}(0)$ is

$$g^{(2)}_{2D}(0)=\frac{N_{TR}}{N_{T\ vs}N_R}\left(\frac{\Delta T}{\Delta t}\right). \tag{11}$$

N_R is not replaced by $N_{R\ vs}$ because the R detector is connected to the STOP input of the TAC. Once the START circuitry of the TAC has been initiated, any detection at R can trigger the STOP and hence determine a coincidence.

Now consider the effects on $g^{(2)}_{3D}(0)$. For these measurements three coincidences are needed, so three TACs are used. The denominators used to calculate the coincidence probabilities in Eq. (9) should be replaced by the corresponding number of VSs. The correct expressions are then

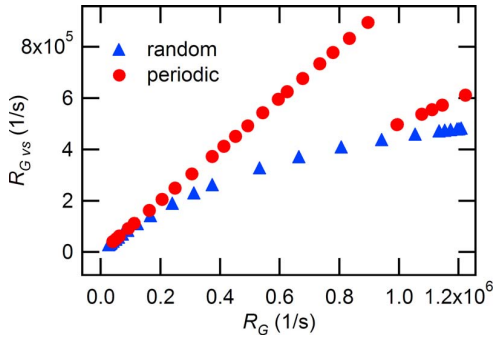

Fig. 3. (Color online) Rate of VALID STARTs on the gate $R_{G\ vs}$ is plotted versus STARTs R_G. Circles are for a periodic train of STARTs, while triangles are for a random stream of STARTs from the downconversion source.

$$P_{GT}=\frac{N_{GT}}{N_{G\ vs}},\quad P_{GR}=\frac{N_{GR}}{N_{G\ vs}}, \tag{12}$$

where $N_{G\ vs}$ is the number of VSs from the TAC measuring GT coincidences. Since the dead times and count rates in the GT and GR TACs are nearly the same, and it is the G detector that acts as the gate, then the number of valid starts for these two TACs are essentially the same (this has been verified experimentally), and one needs only to measure the VSs from one of the TACs.

Notice that the expression for the threefold probability has not been modified. This is because in the experiments it is measured slightly differently. As described in [15], the output of the G detector does not go into the START but rather into the START GATE. The T detector is plugged into the START, and a conversion event is initiated in this TAC when there is a *coincidence* between the G and T detectors. This coincidence rate is over 1 order of magnitude less than the rate at which dead-time effects are important (this has also been experimentally verified.) Thus, dead time has essentially no effect in measuring threefold coincidences, and the expression for the threefold probability is still properly determined using N_G, which initiates everything via the START GATE. Taking all of this into account, the expression for $g^{(2)}_{3D}(0)$ that properly accounts for dead-time effects in the TACs is

$$g^{(2)}_{3D}(0)=\frac{(N_{G\ vs})^2N_{GTR}}{N_GN_{GT}N_{GR}}. \tag{13}$$

The adverse effects of dead time in uncorrected measurements of $g^{(2)}_{2D}(0)$ and $g^{(2)}_{3D}(0)$ [Eqs. (7) and (10)] are demonstrated in Section 4, which presents experimental data. It is also shown that Eqs. (11) and (13) provide a reasonable means to correct for dead-time effects. This is done by comparing corrected measurements performed using TACs to measurements performed using a logic circuit, which has essentially no dead time. When using the logic circuit Eqs. (7) and (10) accurately determine $g^{(2)}_{2D}(0)$ and $g^{(2)}_{3D}(0)$, even at very high count rates.

4. EXPERIMENTS

In these experiments I used single-photon counting modules (SPCMs) based on Geiger mode avalanche photodiodes as the detectors. Coincidences were determined in one of two ways: using a combination of TACs and single channel analyzers (SCAs) or using a logic circuit. The logic circuit used pulse shaping to shorten the ~25 ns output pulses from the SPCMs to ~10 ns, and then performing a logical AND operation on the shortened pulses to determine a coincidence. Details of the circuit will be published elsewhere (see also [18].) Counting was done using a plugin card in a computer, which simultaneously counted on up to eight channels. I used a combination of a half-wave plate and a polarizing beam splitter (PBS) in place of an ordinary beam splitter; this allowed me to adjust the splitting ratio to ensure that the count rates on the T and R detectors were roughly equal. A more detailed description of the experimental procedures can be found in [15,18].

For measurements of $g^{(2)}_{2D}(0)$ it is necessary to measure the coincidence time window Δt. This is done using a source of uncorrelated photons. Light from a 405 nm laser diode is shone on a piece of white paper (placed directly behind the downconversion crystal in Fig. 2.) Scattered light passes through the beam splitter and is detected at detectors T and R. Although the SPCMs have RG780 filters that block wavelengths shorter than 780 nm, the laser is intense enough to generate enough scattered photons to perform this calibration. Additionally, the laser also produces some florescence above 780 nm, which contributes to the calibration measurement. The assumption when performing this calibration is that any coincidence detections between T and R are uncorrelated and are due to random chance [i.e., that $g^{(2)}_{2D}(0)=1$.] To calibrate the logic circuit Eq. (7) is used, and the temporal resolution was found to be $\Delta t=6.57\pm0.04$ ns. The coincidence window for the TAC experiments was calibrated using Eq. (11) and was adjusted to be close to that of the logic circuit, $\Delta t=6.83\pm0.04$ ns. These results are consistent with coincidence resolution measurements obtained using a delay generator.

A. Two-Detector Measurements

I have measured $g^{(2)}_{2D}(0)$ for a single beam (the signal beam) of a spontaneous parametric downconversion source. The experimental arrangement is shown in Fig. 2. The source was a 3-mm-long crystal of beta-barium borate pumped by a 180 mW, 405 nm laser diode. The geometry was noncollinear, type I downconversion. Since in two-detector measurements there is no gating on the presence of a photon in the idler beam, the field striking the beam splitter is not prepared in a single-photon state but should instead behave like a classical, thermal source for which one expects $g^{(2)}_{2D}(0)=2$. However, if one examines the full temporal behavior of $g^{(2)}(\tau)$ for a thermal source, one finds that it has a constant background of $g^{(2)}(\tau)=1$, but there is a "bump" that rises to $g^{(2)}(\tau)=2$ at $\tau=0$ [13,14,19]. The temporal width of this bump is on the order of the coherence time of the source. If the temporal resolution of the coincidence measurement is much larger than this coherence time, then the bump cannot be resolved, so one expects to measure $g^{(2)}_{2D}(0)\cong1$ [13,14]; this is certainly the case in this experiment, since the coherence time is less than 100 fs, and the coincidence resolution is >1 ns.

In Fig. 4(a) I show plots of $g^{(2)}_{2D}(0)$ versus the average count rate measured at detector T, R_T; the data was obtained using a TAC. Each point represents the average of 10 measurements with $\Delta T=30$ s. Results are shown for calculations of $g^{(2)}_{2D}(0)$ using Eqs. (7) and (11). It is seen that calculating $g^{(2)}_{2D}(0)$ using Eq. (11), which corrects for dead-time errors, yields the expected result of $g^{(2)}_{2D}(0)=1$ for all count rates. Equation (7), however, erroneously indicates that $g^{(2)}_{2D}(0)$ decreases with increasing singles count rate, because the TR coincidences are being undercounted owing to dead time effects.

In Fig. 4(b) I compare measurements obtained using the TAC [and Eq. (11)] and the logic circuit [and Eq. (7)]. The error bars come from two sources. The first is simply the statistical error of the measurements (the standard deviation of 10 measurements with $\Delta T=30$ s); this error dominates at the lower count rates. The other source of error is the uncertainty in the coincidence time resolution that is used to calculate $g^{(2)}_{2D}(0)$; this error dominates at the higher count rates. It is seen that all of the data is consistent with $g^{(2)}_{2D}(0)=1$, indicating that (i) the logic circuit does not suffer from dead time errors, and (ii) Eq. (11) reasonably corrects for dead-time errors when using a TAC.

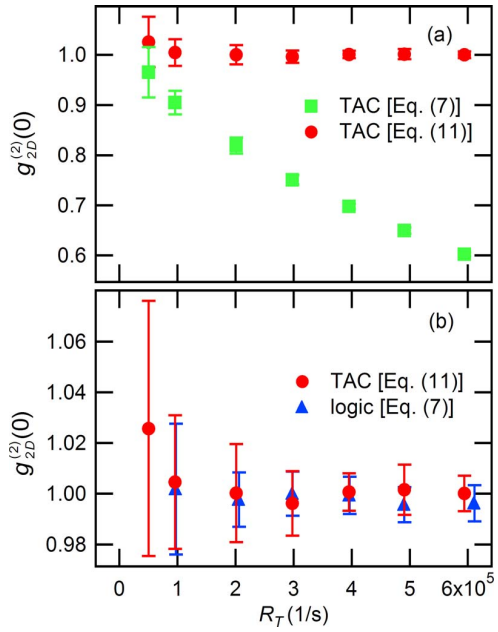

Fig. 4. (Color online) The degree of second-order coherence measured with two detectors $g^{(2)}_{2D}(0)$ is plotted versus the singles rate on detector T, R_T. The sources of error are described in the text. In (a) data taken using the TAC is compared for analysis using Eqs. (7) and (11). In (b) data acquired using the TAC and the corrected expression Eq. (11) is compared to data acquired using the logic circuit and the uncorrected expression Eq. (7).

B. Three-Detector Measurements

As described above in Section 2, detection of a photon in the idler beam by the gate detector projects the signal beam into a single-photon state. This is an inherently quantum-mechanical state and allows the observation of $g^{(2)}_{3D}(0)<1$. This effect has been seen before (see, for example, [5,15]), and the purpose here is to determine how this observation is affected by dead time.

In Fig. 5 I show measured values of $g^{(2)}_{3D}(0)$ as functions of the singles count rate on the gate detector R_G; each point represents the average of 10 measurements with $\Delta T=30$ s. The statistical error of each point is smaller than the size of the corresponding marker. At the lowest count rates all of the measurements yield $g^{(2)}_{3D}(0)<0.035$, but in each situation the values of $g^{(2)}_{3D}(0)$ increase with R_G. The values for $g^{(2)}_{3D}(0)$ obtained using the TAC and Eq. (10) grow the most rapidly and eventually exceed one; the primary reason for this increase in $g^{(2)}_{3D}(0)$ is dead-time effects, and hence these values are erroneous.

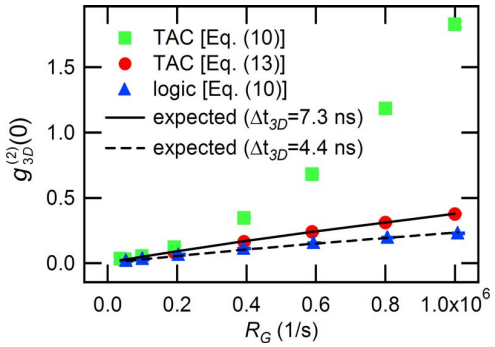

Fig. 5. (Color online) The conditional degree of second-order coherence measured with three detectors $g_{3D}^{(2)}(0)$ is plotted versus the singles rate on detector G, R_G. Markers represent data taken using the TAC and analyzed using Eqs. (10) and (13) and also data taken using the logic circuit. Error bars (representing the standard deviation of 10 measurements) are smaller than the markers. Lines represent the expected value of $g_{3D}^{(2)}(0)$ determined using Eq. (14) for two different values of Δt_{3D}.

In Fig. 5 the values for $g_{3D}^{(2)}(0)$ obtained using the logic circuit and those obtained using the TAC and Eq. (13) increase owing to increasing accidental coincidence rates. In [15] it was shown that the expected measured value for $g_{3D}^{(2)}(0)$ when accidental coincidences are accounted for is

$$g_{3D}^{(2)}(0) = R_G \Delta t_{3D} \left(\frac{R_R}{R_{GR}} + \frac{R_T}{R_{GT}} \right). \tag{14}$$

The primary assumption made in deriving this expression was that the accidental threefold detections come primarily from a true twofold coincidence, and then an accidental detection at the third detector within a time window of Δt_{3D} (this time window need not be the same as the time window for the two detector measurements—although it will ordinarily be on the same scale). This time interval cannot be directly measured using uncorrelated photons (since the assumption is that there is a valid twofold coincidence, and uncorrelated photons do not produce such a coincidence); one way to determine it is to fit the measured $g_{3D}^{(2)}(0)$ data using Eq. (14) with Δt_{3D} as the fit parameter. The lines in Fig. 5 show plots of Eq. (14) for two different values of Δt_{3D}: Δt_{3D}=4.4 ns, appropriate for the logic circuit, and Δt_{3D}=7.3 ns, appropriate for the TAC and Eq. (11). It is seen that with the correct value for Δt_{3D}, Eq. (14) accurately determines $g_{3D}^{(2)}(0)$ from the expected accidental threefold coincidences.

I note that in [15] Eq. (10) was used to calculate $g_{3D}^{(2)}(0)$, instead of the corrected expression in Eq. (13). What effect did this have on the values of $g_{3D}^{(2)}(0)$ reported there? The values for $g_{3D}^{(2)}(0)$ in Eqs. (10) and (13) differ by a factor of $(N_{G\ vs}/N_G)^2$, which for the count rates in [15] is about 0.8. Thus the corrected values for $g_{3D}^{(2)}(0)$ would be smaller than reported in [15] by this factor.

5. CONCLUSIONS

These experiments yield several insights. The first is that dead-time effects in a TAC can lead to erroneous measurements of $g_{2D}^{(2)}(0)$ and $g_{3D}^{(2)}(0)$. The ideal solution to this problem is to use equipment for coincidence determination that reduces dead time. I have shown that a high-speed logic circuit does exactly this. When using this circuit it is possible to use the well-known expressions for $g_{2D}^{(2)}(0)$ and $g_{3D}^{(2)}(0)$ [Eqs. (7) and (10)] and still obtain accurate results. Since the logic circuit operates at higher count rates, has comparable time resolution, and is much less expensive than the TACs, it is the superior instrument for these measurements.

The second insight is that it is possible to mitigate dead time effects in such measurements by counting the VALID STARTS from the TACs and using Eqs. (11) and (13) to calculate $g_{2D}^{(2)}(0)$ and $g_{3D}^{(2)}(0)$. These corrected measurements yield much better agreement between experiment and theory. Thus, if measurements must be performed using TACs the renormalized expressions derived here will be of use to experimenters.

ACKNOWLEDGMENTS

I thank R. Haskell for inspiring me to examine the questions addressed here, as well as for numerous helpful conversations. I also thank S. Bhandari, D. Branning, and L. North for their help with the logic circuit. This project was carried out with the support of the National Science Foundation and Whitman College.

REFERENCES AND NOTES

1. R. Hanbury Brown and R. Q. Twiss, "Correlation between photons in two coherent beams of light," Nature (London) **177**, 27–29 (1956).
2. R. Q. Twiss, A. G. Little, and R. Hanbury Brown, "Correlation between photons in coherent beams of light, detected by a coincidence counting technique," Nature (London) **180**, 324–326 (1957).
3. H. J. Kimble, M. Dagenais, and L. Mandel, "Photon antibunching in resonance fluorescence," Phys. Rev. Lett. **39**, 691–695 (1977).
4. Some references use the normalized intensity correlation function $\lambda(\tau)$ in place of the degree of second-order coherence; they are related by $g^{(2)}(\tau)=1+\lambda(\tau)$.
5. P. Grangier, G. Roger, and A. Aspect, "Experimental evidence for a photon anticorrelation effect on a beam splitter: a new light on single-photon interferences," Europhys. Lett. **1**, 173–179 (1986).
6. P. G. Kwiat and R. Y. Chiao, "Observation of a nonclassical Berry phase for the photon," Phys. Rev. Lett. **66**, 588–591 (1991).
7. S. Fasel, O. Alibart, S. Tanzilli, P. Baldi, A. Beveratos, N. Gisin, and H. Zbinden, "High-quality asynchronous heralded single-photon source at telecom wavelength," New J. Phys. **6**, 163 (2004).
8. C. W. Chou, S. V. Polyakov, A. Kuzmich, and H. J. Kimble, "Single-photon generation from stored excitation in an atomic ensemble," Phys. Rev. Lett. **92**, 213601 (2004).
9. T. Chaneliere, D. N. Matsukevich, S. D. Jenkins, S. Y. Lan, T. A. B. Kennedy, and A. Kuzmich, "Storage and retrieval of single photons transmitted between remote quantum memories," Nature (London) **438**, 833–836 (2005).
10. A. B. U'Ren, C. Silberhorn, J. L. Ball, K. Banaszek, and I. A. Walmsley, "Characterization of the nonclassical nature of conditionally prepared single photons," Phys. Rev. A **72**, 021802(R) (2005).
11. C. Santori, S. Gotzinger, Y. Yamamoto, S. Kako, K. Hoshino, and Y. Arakawa, "Photon correlation studies of single GaN quantum dots," Appl. Phys. Lett. **87**, 051916 (2005).
12. E. Wu, V. Jacques, H. P. Zeng, P. Grangier, F. Treussart,

and J. F. Roch, "Narrow-band single-photon emission in the near infrared for quantum key distribution," Opt. Express **14**, 1296–1303 (2006).
13. R. Loudon, *The Quantum Theory of Light*, 3rd ed. (Clarendon, 2000).
14. L. Mandel and E. Wolf, *Optical Coherence and Quantum Optics* (Cambridge U. Press, 1995).
15. J. J. Thorn, M. S. Neal, V. W. Donato, G. S. Bergreen, R. E. Davies, and M. Beck, "Observing the quantum behavior of light in an undergraduate laboratory," Am. J. Phys. **72**, 1210–1219 (2004).
16. C. K. Hong and L. Mandel, "Experimental realization of a localized one-photon state," Phys. Rev. Lett. **56**, 58–60 (1986).
17. I am not alone in associating α and $g^{(2)}(0)$; see also the text by Loudon [13]. It is reasonable for one to think of the three-detector $g^{(2)}(0)$ as being a third-order intensity correlation. However, I prefer to follow Loudon's lead and consider it a conditional $g^{(2)}(0)$.
18. M. Beck, "Modern quantum mechanics experiments," http://www.whitman.edu/~beckmk/QM/.
19. F. T. Arecchi, E. Gatti, and A. Sona, "Time distribution of photons from coherent and Gaussian sources," Phys. Lett. **20**, 27–29 (1966).